Indonesian Journal of Aerospace Vol. 23 No. 1 Juni 2025 : pp 1 – 12 (Rozzykin et al.)
DOI: 10.59981/ijoa.2025.5055
https://ejournal.brin.go.id/ijoa/

Potentially Habitable Terrestrial Exoplanets based on the Habitability Index for Transiting Exoplanets (HITE) Value

Achmad Zainur Rozzykin[1,2], Claudia Amelia Lomban[1], M. Isnaenda Ikhsan[1,2]

[1]Department of Atmospheric and Planetary Sciences, Faculty of Science, Sumatera Institute of Technology, South Lampung, Lampung, Indonesia
[2]Planetary and Space Sciences Research Group, Faculty of Science, Sumatera Institute of Technology, South Lampung, Lampung, Indonesia
e-mail: achmad.rozzykin@sap.itera.ac.id

Received: .13-06-2025. Accepted: 17-07-2025 Published: 05-10-2025

Abstract

In-depth exploration of exoplanet habitability involves a crucial screening process to identify a subset with the potential for sustaining life. The Habitability Index for Transiting Exoplanets (HITE) emerges as a vital tool, quantifying a planet's habitability by assessing the probability of it having a solid surface and liquid water. Represented by the symbol H, the index assigns values on a scale from 0 to 1. The closer the value to 1, the greater the potential for habitability. H integrates parameters derived from transit data, encompassing orbital period, transit depth, duration, surface gravity, radius, and effective temperature of the host star. Through the Virtual Planetary Laboratory (VPL), the calculation of H is executed for exoplanets with terrestrial mass (0.3–10 M⊕) sourced from the Transiting Exoplanet Survey Satellite (TESS) and K2 missions. The results show that the exoplanets with the highest H values are TOI-700 d from TESS, with a value of 0.95202. Of the 228 planets examined, around 9.21% are identified as potentially habitable.

Keywords: *HITE; exoplanet; terrestrial; transit; habitable planet*

1. Introduction

Since the discovery of the first exoplanet orbiting a Sun-like star in 1995, the field of exoplanet research has grown rapidly. The number of confirmed and potential exoplanets, the techniques used to detect and study them, and the amount of data collected from space missions and ground-based telescopes have all increased significantly. Many researchers have contributed to compiling and sharing information about exoplanets, making it accessible to both scientists and the public. Resources like the Extrasolar Planet Encyclopedia and the Exoplanet Orbit Database provide detailed information on confirmed and retracted exoplanets, as well as those with well-defined orbits. Additionally, archives from space missions like Kepler and CoRoT, along with services like the Exoplanet Transit Database, offer valuable data and tools for exoplanet research (Akeson et al., 2013).

The habitable zone (HZ) is a circumstellar region where liquid water could exist on a rocky planet's surface. Primarily used for mission planning, the HZ guides the selection of planetary targets for further investigation. While a planet within the HZ doesn't guarantee habitability, it remains the most effective tool for identifying potentially life-sustaining worlds (Ramirez, 2018). The habitable zone distance consists of two types, namely the conservative habitable zone and the optimistic habitable zone. The conservative habitable zone has an outer boundary, which is defined as the place where condensation and scattering by CO_2 exceed the capacity of the greenhouse, so it is called the maximum greenhouse limit, while the inner boundary is defined as the situation where the average surface temperature exceeds the water critical point, triggering an uncontrolled greenhouse that causes water to evaporate in the form of H_2O in a very short time span. For the optimistic habitable zone, the boundary within the habitable zone corresponds to the initial Venus boundary based

on the condition that liquid water has not existed on Venus for at least 1 Gyr, and the limit of the existence of water on the planet's surface is seen from the beginning of the planet's formation. The outer boundary is based on the early Martian region, which is a region dense in CO_2 and warm enough for liquid water to flow on the planet's surface (Yustika et al., 2021). For a planet to be habitable on the surface, it must be within the habitable zone flux boundary and terrestrial (Barnes et al., 2015). Both conditions can be met based on available transit data.

Terrestrial planets have the main composition of rock, silicate, water, metal, and/or carbon. Based on their mass and radius, terrestrial planets are divided into sub-terran planets, terran planets, and superterran planets. Table 1-1 shows the detailed classification of terrestrial planets.

Table 1-1: Classification of Terrestrial Planets

Type	Mass (M⊕)	Radius (r⊕)
Sub-terran	0.0194	0.8481
Terran	0.0165	1.4530
Super-terran	0.0150	2.8793

The transit method is one way to find exoplanets. From exoplanet transit data, parameters can be obtained that can be used to estimate the properties of the planet. The Habitability Index for Transiting Exoplanets (HITE) value (Barnes et al., 2015) can be used to determine whether an exoplanet can be considered habitable. The habitability potential is obtained by calculating the probability that a planet has a solid surface and liquid-phase water on the surface. The closer the index value is to 1, the more potentially habitable it is based on several parameters, namely orbital period P, transit depth d, transit duration D, surface gravity of the host star g, radius of the parent star r*, effective temperature of the parent star T*, and impact parameters b.

This research takes confirmed exoplanet transit data from the Transiting Exoplanet Survey Satellite (TESS) mission and additionally K2 as a follow-up mission from Kepler. Terrestrial mass planets (0.3–10 M⊕) are included in the search for habitable exoplanets; an orbital period of greater than 10 days is necessary for planets whose mass is unknown. The aim of this research is to determine terrestrial exoplanets that are potentially habitable by calculating the HITE value of terrestrial exoplanets from the TESS and K2 missions, then comparing the number of terrestrial exoplanets that are potentially habitable and those that are not habitable.

2. Methodology

Exoplanet transit data were taken from the NASA Exoplanet Archive (NASA Exoplanet Science Institute, n.d.), and gaps were supplemented by the Exo.MAST (Mikulski Archive for Space Telescopes) catalog (Space Telescope Science Institute, n.d.). Then the HITE value calculation is carried out via the HITE Virtual Planetary Laboratory (VPL) website (Barnes et al., n.d.).

The transit method represents a simple way to detect planets. If a planet passes in front of its parent star from the observer's perspective, the star will show brief and periodic dimming, indicating the presence of a planet. Transit occurs when the planet's orbital impact parameters with respect to the host star are in radius units. The impact parameter b is defined as the distance projected in the sky between the center of the star disk and the center of the planet disk at the time of conjunction, as formulated in Eq. (2-1) (Stephan & Gaudi, 2023).

$$b \equiv \frac{a \cos i}{r} \frac{1 - e^2}{1 + e \sin \omega_*} \quad (1)$$

Transit is characterized by transit duration D, ingress/egress time τ, and transit depth d. The transit depth is relative to the flux outside the transit, as seen in Eq. (2-2) (Stephan & Gaudi, 2023).

$$d = \frac{F_{no\ transit} - F_{transit}}{F_{no\ transit}} \quad (2)$$

Eq. (2-3) can be used to estimate the planet's radius based on the relationship between transit depth and radius.

$$r_p = \sqrt{d r_*^2} \quad (3)$$

The transit and star data give the planet's radius R_p, but not the planet's mass M_p or the star's mass M_* so the mass needs to be determined in another way. The mass of the star is estimated in Eq. (2-4) (Barnes et al., 2015).

$$M_* = \frac{10^{log\ g}\, r_*^2}{G} / 100 \quad (4)$$

G is the universal gravitational constant equal to 6.6728×10^{-11} m^3/kgs^2, log g in units of cm/s^2, and r_* in units of meters.

Modeling based on the composition of Earth-like planets (Beltzer & Miranda, 2023) is one of the mass-radius relationships of terrestrial planets and is displayed in Eq. (2-5).

$$\frac{M_p}{M_\oplus} = 1,46 \left(\frac{r_p}{r_\oplus} \right)^{2.6} \quad (5)$$

The HITE calculation steps begin with calculating the flux limit, minimum eccentricity, maximum eccentricity, eccentricity distribution, terrestrial conditions, and eccentricity-albedo degeneration. Then the HITE value can be calculated, which is symbolized by H.

The flux value F depends on the luminosity L_*, semi-major axis a, albedo A, and eccentricity e, and is defined by Eq. (2-6) (Barnes et al., 2015).

$$F = \frac{L_*(1 - A)}{16\pi a^2 \sqrt{1 - e^2}} \quad (6)$$

Luminosity L_* is the total energy emitted by a star per second within a spherical surface area, calculated from radius r, temperature T, and based on the Stefan-Boltzmann Law shown in Eq. (2-7).

$$L_* = 4\pi r_*^2 \sigma T_*^4 \quad (7)$$

The semi-major axis a is calculated from its relationship with the period P in Kepler's 3rd Law, shown in Eq. (2-8).

$$a = \sqrt[3]{G(M_* + M_p)/4\pi^2 P^2} \quad (8)$$

Eq. (2-9) illustrates the effective insolation received by the planet at a given distance based on the luminosity and semi-major axis.

$$S_{eff} = \frac{L_*}{4\pi a^2} \quad (9)$$

The F_{max} value is determined by a process called the runaway greenhouse effect. There comes a point at which the atmosphere becomes optically thick to infrared radiation, decoupling the surface temperature from a fixed photospheric temperature, as high surface temperatures render water vapor a nonnegligible component of the atmosphere. A planet's water inventory evaporates into the atmosphere if its instellation is greater than this value, and eventually the planet is driven into space by photodissociation and atmospheric escape. Below this threshold, significant water vapor escape is also possible. The stratospheric water vapor level quickly rises by orders of magnitude near the "moist greenhouse" limit, resulting in the loss of water equivalent to the entire Earth's surface over hundreds of megayears (Innes et al., 2023). The analytical greenhouse flux limit is shown in Eq. 10 (Barnes et al., 2015).

$$F_{max} = B\sigma\left(\frac{l}{2R\,ln(p_*\sqrt{k}p_0 g)}\right)^4 \quad (10)$$

B is the unitary coefficient to fit the detailed radiative transfer model, σ is the Stefan–Boltzmann constant, l is the latent heat capacity of water, R is the universal gas constant, p_0 is the pressure at which the water vapor line strength is evaluated, k is the gray absorption coefficient, and g is the gravitational acceleration on the surface given by mass and radius in Eq. (2-11).

$$g = G\frac{M}{r^2} \quad (11)$$

Large eccentricities in multiplanetary systems have the potential to induce dynamic instability and planetary system destruction. The minimum eccentricity value can be derived by comparing D with the expected duration if the planet were in a circular orbit, D_c which is expressed in Eq. (2-12) (Barnes et al., 2015).

$$D_c = \frac{\sqrt{(r_* + r_p)^2 - b^2}}{\pi a} P \quad (12)$$

The transit duration anomaly is shown as $\Delta \equiv D/D_c\, \Delta \equiv D/D_c$. When combined with Kepler's Second Law, the minimum eccentricity of the emin can be determined in Eq. (2-13) (Barnes et al., 2015).

$$e_{min} = \left|\frac{\Delta^2 - 1}{\Delta^2 + 1}\right| \quad (13)$$

The maximum eccentricity is estimated with the Gladman formalism and Hill stability, which requires Eq. (2-14).

$$e_{min} = \left|\frac{\Delta^2 - 1}{\Delta^2 + 1}\right| \quad (14)$$

where $\mu_i = \frac{m_i}{M_*}$; $\zeta = \mu_1 + \mu_2$; $\gamma_i = \sqrt{1 - e_i^2}$; and $\lambda = \sqrt{\frac{a_{out}}{a_{in}}}$. The subscript i denotes a planet, M_* is the mass of the star, and a_{in} and a_{out} are the semi-major axes of the inner and outer planets, respectively. Eq. (2-15) gives the maximum eccentricity (Barnes et al., 2015).

$$e_{max} = \sqrt{1 - \left(\frac{\sqrt{\left(\frac{1 + \sqrt[3]{3^4}\left(\frac{\mu_1\mu_2}{\sqrt[3]{\zeta^4}}\right)}{\zeta^{-3}\left(\mu_1 + \frac{\mu_2}{\lambda^2}\right)}\right)} - \mu_2\gamma_2\lambda}{\mu_1}\right)^2} \quad (15)$$

Verifying if the exoplanet is terrestrial or has a solid surface is among the most crucial tasks. Eq. (2-16) models the chance of a planet being non-gaseous (Barnes et al., 2015).

$$\begin{aligned} &1, r_p \le 1.5r\oplus, \\ &P_{rocky}(r_p) = (2.5 - r_p), \quad 1.5r\oplus < r_p < 2.5r\oplus, \\ &0,\ r_p \ge 2.5r\oplus \end{aligned} \quad (16)$$

An assessment scheme for potentially habitable planets is developed by combining all of these ideas. Eq. (2-17) first establishes the intermediate parameter h,

$$h(A,e) = 1,\ F_{min} < F < F_{max} \quad \textbf{(17)}$$
$$0,$$

with the limit $0.05 \leq A \leq 0.8$ and $e_{min} \leq e \leq e_{max}$. If h = 1 it is likely that the planet is terrestrial. Next, the HITE value can be calculated using Eq. (2-18),

$$\boldsymbol{H = \frac{\Sigma h_j p_j(e)}{\Sigma p_j(e)} p_{rocky}} \quad \textbf{(18)}$$

Where j is the index (A, e), and $p_j(e)$ is the eccentricity probability distribution (Barnes et al., 2015).

3. Result and Analysis

Whereas the masses in the NASA Exoplanet Archive catalog have been verified by other techniques, the mass calculations on the VPL HITE website rely solely on transit data. Furthermore, an exoplanet with an unknown mass could have a mass greater than 10M⊕, in which case it would not be classified as a terrestrial planet or as a Neptune-like planet (10M⊕-100M⊕) (Yustika et al., 2021). HITE relies on strong assumptions and limited data. Transit observations constrain period and radius but not eccentricity or albedo, so Barnes et al. adopt broad priors and empirical eccentricity distributions. This "eccentricity–albedo degeneracy" means different (e, A) combinations can fit the data, undermining precision. Likewise, radius alone cannot confirm a rocky composition; HITE downweights large planets as likely "mini-Neptunes," but the 1.5 R⊕ - 2 R⊕ cut-off is uncertain. HITE also assumes Earth-like climate physics: it uses analytic runaway-greenhouse limits and ignores clouds or atmospheric composition differences. In sum, HITE's conceptual weaknesses include oversimplified climate thresholds and unknown albedo, while its methodological limits stem from sparse transit data (missing density, atmosphere, geochemistry) and the need to impose arbitrary priors (Barnes et al., 2015). These factors mean HITE can rank candidates but cannot guarantee true habitability – it highlights comparative potential rather than definitive criteria.

Transit surveys like Kepler, K2, and TESS are inherently biased toward short-period, large planets. As Jiang et al. (2024) note, the transit method disproportionately finds planets with short orbital periods, because these yield more frequent, detectable transits. This over-samples "hot" worlds very close to their stars, skewing habitability statistics. For example, Kepler/K2 almost never detects Earth-analogs at 1 AU, and TESS's 27-day per-sector baseline makes 365-day orbits essentially undetectable except in the continuous-view zones. Conversely, the radial-velocity (RV) method finds only massive, Jupiter-like planets. These detection biases directly affect habitability assessments. Since known planets are overwhelmingly close-in super-Earths or Neptunes, any HITE or habitability index computed on the sample will be biased. Inferences about the true distribution of habitable worlds must thus correct for these selection effects. Put simply, the observational pipeline (transit geometry, mission duration, detection threshold) imposes a bias in the sample of available planets, which must be considered when applying HITE or other indices to assess habitability.

Table 3-1 displays the list of exoplanets from this study that may be habitable. TOI-700 d from the TESS mission has the greatest possible habitability rankings. Understanding the planetary system, composition, environment, and atmosphere of a planet is necessary to confirm whether exoplanets are habitable.

The main possibly habitable exoplanets are shown in Figure (3-1) and (3-2) to be located in the semi-major axis of less than 0.2 AU and to be orbiting class M stars, or stars with a temperature between 3000 and 4000 K. It is still possible for a host star with a lower temperature than our Sun to be habitable on exoplanets with low semi-major axes.

When a planet's emission reaches the feasible limit for the habitable zone, it is said to be livable. For all terrestrial planets, the flux limit is F_{min} = 67 W/m^2 (Barnes et al., 2015). For aquatic planets, the alternative F_{max} is 330 W/m^{2,} and for terrestrial planets, 415 W/

m^2. Exoplanets with high H values in Figure (3-3) are getting closer to 330 W/m^2 as their maximum flux. Exoplanets that are dry or aquatic may or may not be habitable, while dry planets typically have low H values. H will be high at not very high fluxes for aquatic worlds at the outer limit of the habitable zone because the available energy may be insufficient to prevent glaciation or freezing of the planet. However, because there is less water available for clouds, snow, and ice, land planets are more resilient to global freezing. Low-tilt land planets are frozen at 77% and aquatic worlds at 90% near the outer boundaries (Abe et al., 2011).

TOI-700 d has an H of 0.95202 and receives a flux from its star of about 0.86 ± 0.2 of Earth's insolation flux, which places it within the conservative outer edge habitable zone (Gilbert, et. al., 2020) and can be seen in Figure (3-4). The green area indicates a conservative habitable zone, and further in is an optimistic habitable zone. This result is consistent with earlier studies that found that for F < 415 W m^{-2}, a 1 $M_{\oplus}$ planet might be habitable (Abe et al., 2011).

TOI-700 d has the greatest H value of the 21 exoplanets with values larger than zero; its value would even surpass Earth's H value of 0.829 if transit observations are conducted. However, this does not imply that this planet is 'more habitable' than Earth. This indicates that the twin planet of Earth circles the twin host star of the Sun. The application of HITE to the exoplanets found by Kepler demonstrated the same thing. Among them is Kepler-442 b, a confirmed exoplanet with an H value of 0.838 (Barnes et al., 2015).

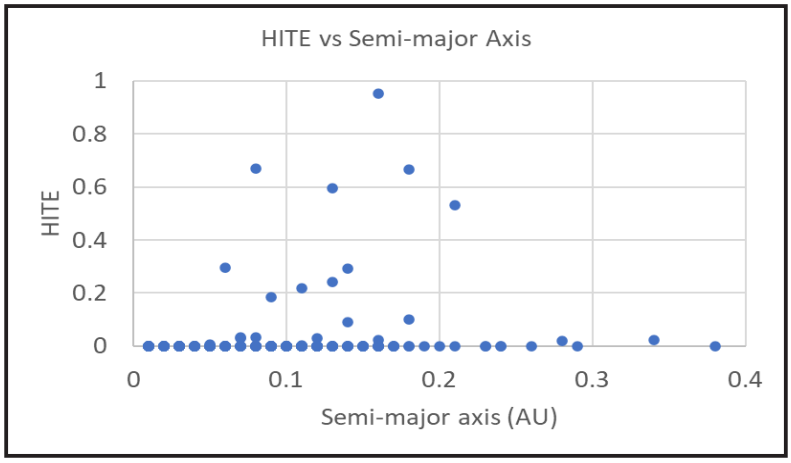

Figure 1: Exoplanet habitability population based on semi-major axis value

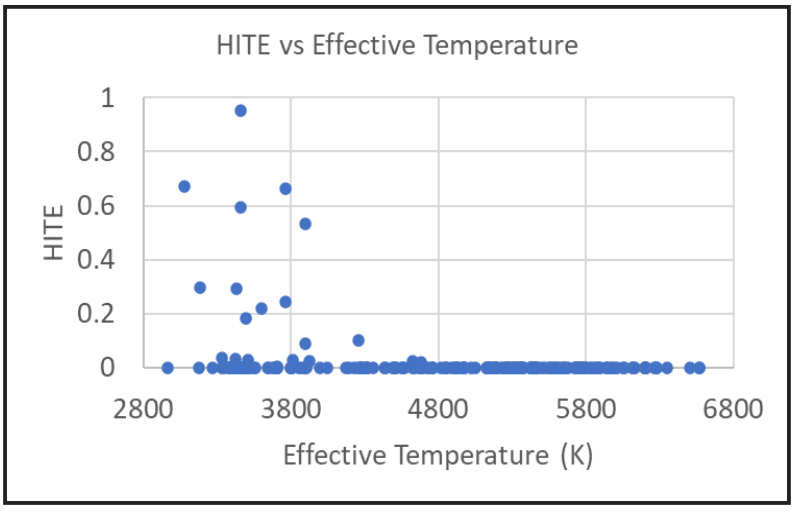

Figure 2: Exoplanet habitability population based on the effective temperature of the host stars

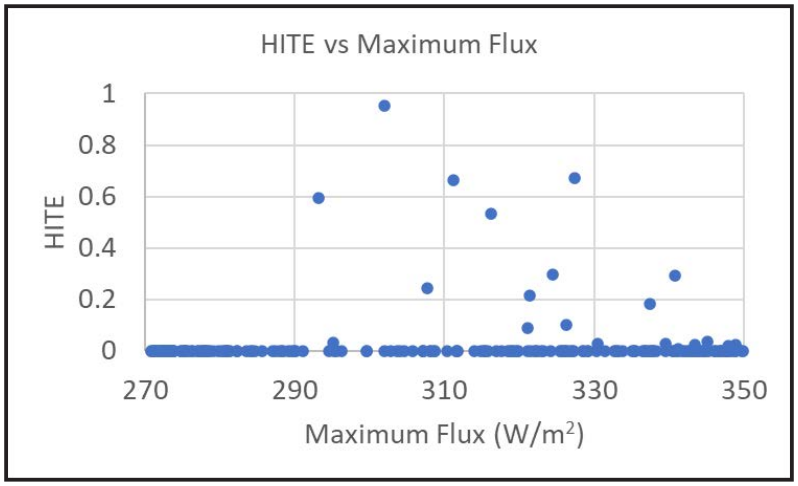

Figure 3: Exoplanet habitability population based on F_{max}

21 exoplanets—or roughly 9.21% of the 228 exoplanets—have an H value > 0 and may be habitable. Just 0.379% of all exoplanets are represented by the 21 potentially habitable exoplanets in this study. Seven planets, or roughly 0.335%, of the 2,086 planets identified in the K2 mission are possibly habitable. On the other hand, we managed to find 14 planets that are possibly habitable, or roughly 3.54%, of the 395 planets confirmed in the TESS mission (Figure (3-5)). Recall that there are only 129 planets in the exoplanets determined by the H value from the TESS mission and 99 planets from the K2 mission.

Unlike Earth Similarity Index (ESI) or Planetary Habitability Index (PHI), which are static similarity or viability scores, HITE is explicitly a probabilistic ranking for transiting planets using only transit and stellar data. HITE incorporates uncertainty (e.g., unknown albedo) by integrating over parameter space, whereas ESI simply plugs in measured values. ESI and PHI assume an Earth-like life paradigm; HITE assumes Earth-like climate limits but then weights by transit-detectable factors (flux and size). In terms of application, ESI and PHI are general conceptual measures (often applied to compare solar-system bodies or to prioritize targets), while HITE is tailored for survey targets: it flags which transiting exoplanets deserve further follow-up (e.g., JWST) based on likely habitability. In short, HITE is a transit-specific probabilistic index, whereas ESI and PHI are phenomenological indices of similarity or life criteria. Each index yields different rankings: for example, a large rocky world may score high on ESI (if similar radius) but low on HITE if it orbits outside the HZ or has a low terrestrial likelihood (Schulze-Makuch et al., 2011).

Atmospheric makeup critically influences surface temperature and thus habitability. Standard habitable zone models assume an Earth-like N_2–CO_2–H_2O atmosphere (or sometimes N_2–CO_2 for outer HZ). In that framework, the inner edge is set by runaway greenhouse (water loss) and the outer edge by CO_2's maximum greenhouse effect. For a Sun-like star, Kopparapu et al. (2013) find these edges at ≈0.99 AU and 1.70 AU. This 1–1.7 AU range assumes moderate CO_2 (scaling with distance) and pressure broadening by N_2. Indeed, enhanced N_2 raises greenhouse warming (via pressure broadening of CO_2/H_2O lines), which can modestly widen the HZ (Goldblatt, et. al., 2009).

By contrast, CO_2-rich or H_2-dominated atmospheres dramatically shift these limits. A dense CO_2atmosphere can keep a planet warm at lower instellation, effectively extending the outer habitable zone. However, at very high CO_2 pressures, the climate may saturate: CO_2 can condense or form reflective clouds, limiting warming. (For example, 1–10 bar CO_2 has been modeled for early Mars; too much CO_2 could trigger glaciation despite its greenhouse effect.) In updated HZ models, the outer edge is indeed set by CO_2's diminishing returns (Kopparapu et al., 2013).

Most strikingly, hydrogen-rich atmospheres enable habitable temperatures far outside the classical HZ. Pierrehumbert & Gaidos (2011) showed that collision-induced absorption in thick H_2–He envelopes produces a powerful greenhouse. Tens of bars of H_2 can maintain liquid-water conditions even under very low flux. Specifically, a 3 M⊕ planet ~40 bar H_2 could be ~280 K at 10 AU from a Sun-like star (and 1.5 AU around an M dwarf.

Table 1: Parameters Used and Obtained for Potentially Habitable Exoplanets

#	Planet name	d (ppm)	P (days)	D (hrs)	b	log g (cm/s^2)	r_* ($r\oplus$)	T_* (K)	M_p ($M_\oplus$)	r_p ($r_\oplus$)	a (AU)	F_{max} (W/m^2)	e_{min}	H
1	TOI-700 d	613	37.42	3.32	0.30	4.81	0.42	3459	1.58	1.13	0.16	302.0122	0.006	0.95202
2	TOI-715 b	4480	19.29	1.98	0.20	5.00	0.24	3075	7.74	1.75	0.08	327.3321	0.038	0.67071
3	TOI-2095 c	772	28.17	3.47	0.10	5.11	0.44	3759	2.86	1.33	0.18	311.138	0.294	0.66508
4	TOI-700 e	433	27.81	2.78	0.47	4.81	0.42	3459	0.85	0.95	0.13	293.1736	0.004	0.59377
5	K2-3 d	590	44.56	4.17	0.30	4.73	0.55	3896	3.95	1.46	0.21	316.287	0.013	0.53135
6	TOI-1452 b	2990	11.06	1.76	0.19	4.95	0.28	3185	6.49	1.67	0.06	324.4089	0.050	0.29484
7	TOI-2257 b	4130	35.19	3.85	0.37	4.97	0.31	3430	16.98	2.17	0.14	340.8465	0.359	0.29075
8	TOI-2095 b	684	17.66	2.61	0.29	5.11	0.44	3759	2.29	1.25	0.13	307.6858	0.209	0.24230
9	TOI-1266 c	1200	18.80	2.19	0.61	4.85	0.42	3600	5.39	1.59	0.11	321.3396	0.012	0.21708
10	TOI-1468 c	3093	15.53	1.76	0.62	5.00	0.34	3496	14.03	2.06	0.09	337.5065	0.040	0.18431
11	K2-155 d	740	40.72	4.46	0.44	4.60	0.58	4258	7.25	1.72	0.18	326.2341	0.051	0.10093
12	K2-3 c	694	24.65	3.43	0.09	4.73	0.55	3896	5.31	1.58	0.14	321.0922	0.031	0.08915
13	LTT 3780 c	3240	12.25	1.39	0.65	4.90	0.37	3331	21.63	2.32	0.08	345.1509	0.199	0.03403
14	K2-239 d	650	10.12	1.84	0.39	4.90	0.36	3420	1.00	1.00	0.07	295.1996	0.006	0.03108
15	TOI-270 d	2640	11.38	2.15	0.23	4.87	0.38	3506	15.77	2.13	0.07	339.5522	0.011	0.02861
16	K2-240 c	980	20.52	3.19	0.29	4.70	0.54	3810	9.32	1.84	0.12	330.4735	0.023	0.02836
17	TOI-712 d	1130	84.84	5.70	0.34	4.64	0.67	4622	26.56	2.46	0.34	348.8607	0.019	0.02347
18	K2-286 b	1120	27.36	3.00	0.35	4.70	0.62	3926	19.69	2.26	0.16	343.4778	0.205	0.02259
19	EPIC 212737443 c	1100	65.55	4.61	0.57	4.62	0.67	4684	25.29	2.42	0.28	347.9704	0.028	0.01921
20	TOI-2136 b	3474	7.85	1.66	0.46	4.91	0.34	3342	17.34	2.19	0.05	341.2258	0.007	0.00603
21	TOI-1470 c	2315	18.09	2.70	0.47	4.77	0.47	3709	16.96	2.47	0.11	349.1293	0.016	0.00383

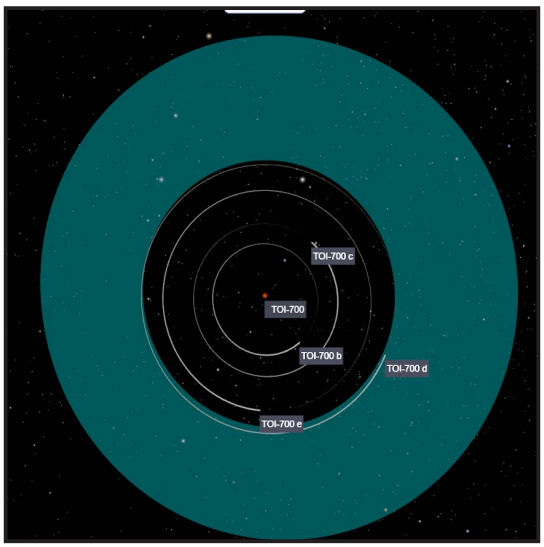

Figure 4: TOI-700 multiplanetary system

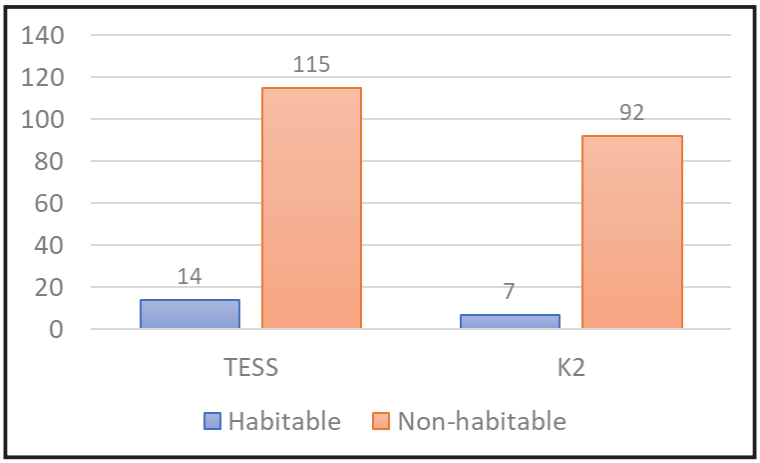

Figure 5: Number of potentially habitable and non-habitable exoplanets from each mission

Such worlds ("Hycean" or mini-Neptune-like) would be considered habitable even though they are far beyond the Earth-Sun HZ. This result implies that planets usually thought to be too cold might sustain warmth if they retain primordial H_2 atmospheres.

In summary, habitability indices based solely on Earth-like atmospheres can misjudge these cases. A planet's ESI or HITE score assumes typical greenhouse behavior, but a CO_2-dominated planet could be habitable outside HITE's nominal habitable zone flux range, and an H_2-enveloped planet could be habitable well below that range. Hence, atmospheric composition is a key uncertainty. Most published HZ boundaries (and thus HITE thresholds) do not apply if the true atmosphere is extremely different from Earth's. Studies explicitly modeling different compositions (e.g., using 1D/3D climate models) show that habitable-zone limits move outward for CO_2-rich cases and vastly outward for H_2 cases (Pierrehumbert & Gaidos, 2011). Any habitability metric or ranking must note these assumptions.

4. Conclusions

This study has applied the Habitability Index for Transiting Exoplanets (HITE) to a sample of 228 terrestrial-mass (0.3–10 M⊕) exoplanets drawn from the TESS and K2 missions, identifying 21 candidates (9.21%) with HITE values greater than zero. Among these, TOI-700 d stands out with an exceptional HITE score of 0.952, placing it well within the conservative habitable-zone boundaries for an M-dwarf host and reinforcing previous validations of its

Earth-like insolation conditions. In aggregate, our results suggest that roughly 0.379% of all confirmed transiting exoplanets to date exhibit conditions marginally consistent with surface liquid water, underscoring both the promise and rarity of potentially habitable worlds in current transit surveys.

However, several key limitations temper these findings. First, HITE's reliance on transit-derived parameters (period, depth, duration, stellar radius, and temperature) necessarily omits direct measurements of planetary mass, eccentricity, atmospheric composition, and albedo—parameters that critically influence surface habitability. The eccentricity-albedo degeneracy and assumptions of Earth-analog greenhouse physics introduce uncertainties that could both under- and overestimate true habitability. Moreover, the intrinsic detection biases of transit surveys—favoring short-period and larger-radius planets—skew the sample away from true Earth analogs at 1 AU, while radial-velocity methods conversely bias toward massive gas giants.

To advance beyond these constraints, future work should integrate multi-method observations: radial-velocity follow-up to constrain masses and densities; transit spectroscopy (e.g., with JWST or upcoming ELTs) to probe atmospheric compositions; and direct imaging to detect reflected light or thermal emission. Incorporating 1D and 3D climate modeling tailored to diverse atmospheric chemistries (CO_2-rich, H_2-dominated, or hybrid mixtures) will refine habitable-zone boundaries and improve indices like HITE. Additionally, as next-generation missions expand the discovery space to longer-period and lower-mass planets, statistical correction for selection effects will be essential to estimate the true occurrence rate of habitable terrestrial worlds.

In conclusion, while HITE provides a practical, probabilistic ranking to prioritize transiting exoplanet targets, it remains a first-order filter rather than a definitive arbiter of habitability. TOI-700 d and its high-scoring peers warrant intensive follow-up, but confirming life-sustaining environments will demand a synthesis of transit data, mass measurements, atmospheric characterization, and detailed climate simulations. By bridging these observational and theoretical approaches, the exoplanet community can move from identifying candidate "Earth-likes" toward assessing their true potential to host life.

Contributorship Statement

AZR analyzed the results and prepared the manuscript; CAL designed the method and analyzed the results; MII analyzed the results.

References

Abe, Y., Abe-Ouchi, A., Sleep, N. H., & Zahnle, K. J. (2011). Habitable zone limits for dry planets. *Astrobiology*, 11(5), 443-460.

Akeson, R. L., Chen, X., Ciardi, D., Crane, M., Good, J., … & Zhang, A. (2013). The NASA Exoplanet Archive: Data and Tools for Exoplanet Research. *Publications of the Astronomical Society of the Pacific*, 125, 990.

Barnes, R., Meadows, V. S., & Evans, N. (2015). Comparative habitability of transiting exoplanets. *The Astrophysical Journal,* 814(2), 91.

Barnes, R., Meadows, V. S., & Evans, N. (n.d.). VPL Habitability Index for Transiting Exoplanets. https://vplapps.astro.washington.edu/hite.php

Betzler, A. S., & Miranda, J. G. (2023). Relation between mass and radius of exoplanets distinguished by their density. *Research in Astronomy and Astrophysics*, 23(6), 065005.

Gilbert, E. A., Barclay, T., Schlieder, J. E., Quintana, E. V., Hord, B. J., Kostov, V. B., ... & Winters, J. G. (2020). The first habitable-zone Earth-sized planet from TESS. I. Validation of the TOI-700 system. *The Astronomical Journal*, 160(3), 116.

Goldblatt, C., Claire, M. W., Lenton, T. M., Matthews, A. J., Watson, A. J., & Zahnle, K. J. (2009). Nitrogen-enhanced greenhouse warming on early Earth. *Nature Geoscience*,

2(12), 891-896.

Innes, H., Tsai, S. M., & Pierrehumbert, R. T. (2023). The Runaway Greenhouse Effect on Hycean Worlds. *The Astrophysical Journal*, 953(2), 168.

Jiang, J. H., Rosen, P. E., Liu, C. X., Wen, Q., & Chen, Y. (2024). Analysis of Habitability and Stellar Habitable Zones from Observed Exoplanets. *Galaxies*, 12(6), 86.

Kopparapu, R. K., Ramirez, R., Kasting, J. F., Eymet, V., Robinson, T. D., Mahadevan, S., Terrien, R. C., Domagal-Goldman, S., Meadows, V., Deshpande, R. (2013). Habitable Zones Around Main-Sequence Stars: New Estimates. https://arxiv.org/abs/1301.6674v2

NASA Exoplanet Science Institute. (n.d.). NASA Exoplanet Archive Data. https://exoplanetarchive.ipac.caltech.edu/

Space Telescope Science Institute. (n.d.). Catalogs: Exoplanet Atmosphere Observability Table. https://catalogs.mast.stsci.edu/eaot

Pierrehumbert, R. & Gaidos, E. (2011). Hydrogen Greenhouse Planets Beyond the Habitable Zone. https://arxiv.org/abs/1105.0021v1

Ramirez, R. M. (2018). A more comprehensive habitable zone for finding life on other planets. *Geosciences*, 8(8), 280.

Schulze-Makuch, D., Méndez, A., Fairén, A. G., von Paris, P., Turse, C., Boyer, G., Davila, A. F., de Sousa António, M. R., Catling, D., & Irwin, L. N. (2011). A two-tiered approach to assessing the habitability of exoplanets. *Astrobiology*, 11(10), 1041-52.

Stephan, A. P., & Gaudi, B. S. (2023). Exoplanet Nodal Precession Induced by Rapidly Rotating Stars: Impacts on Transit Probabilities and Biases. *The Astrophysical Journal*, 950(1), 32.

University of Rochester. (n.d.). A Runaway Greenhouse Effect. https://www.pas.rochester.edu/~blackman/ast104/vgreenhouse.html

Yustika, S. I., Utama, J. A., Arifin, M., Rusdiana, D. (2021). Karakteristik Eksoplanet Laik Huni di Sistem Multiplanet. *Prosiding Seminar Nasional Fisika 7.0*.